ACS APPLIED MATERIALS & INTERFACES

Research Article

www.acsami.org

Visible Light Photocatalytic Degradation of RhB by Polymer-CdS Nanocomposites: Role of the Host Functional Groups

Bingcai Pan,*[,†,‡] Yingmei Xie,[†] Shujuan Zhang,[†] Lu Lv,[†,‡] and Weiming Zhang[†,‡]

[†]State Key Laboratory of Pollution Control and Resource Reuse, School of the Environment, Xianlin Campus, Nanjing University, Nanjing 210093, P.R. China

[‡]National Engineering Center for Organic Pollution Control and Resource Reuse (Suzhou Division), Suzhou High-Tech Institute of Nanjing University, Suzhou 215123, P.R. China

Supporting Information

ABSTRACT: Surface groups of the host polystyrene beads play an important role in the properties of the polymer-based nano-CdS composites in terms of the distribution, dispersion, crystal structure, pH-dependent stability of nano-CdS, and thereafter affect their photocatalytic activity. Surface modification of the host materials can be taken as an effective and general approach to mediate the structure and properties of the nanocomposite materials.

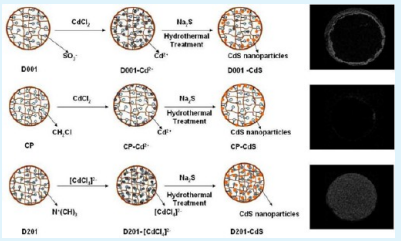

KEYWORDS: *nano-CdS, polystyrene, nanocomposite, functional groups, photocatalytic activity*

1. INTRODUCTION

Heterogeneous photocatalysis has been regard as an attracting option for removing organic contaminants from aqueous or gaseous environment,[1−3] and the widely used photocatalysts generally include metal oxide or sulfide semiconductors, such as TiO_2,[4,5] ZnO,[6,7] Cu_2O,[8,9] CdS,[10] Fe_2O_3,[11] SnO_2,[12] WO_3,[13,14] and Bi_2WO_6.[15] Among them, CdS is one of the most promising photocatalysts that can utilize sunlight as a light source for photocatalytic reactions because of its relatively narrow band gap (2.4 eV).[16]

Traditionally, CdS is applied directly in a suspended system of a remarkable reaction rate. This might be partially attributed to the well-dispersed ultrafine CdS particles of high surface area and reactivity in the receiving water. However, CdS is prone to photocorrosion in oxygen-containing aqueous media during photochemical reaction,[17] and its ultrafine particles result in difficult separation when concerning the practical application. To overcome the above problems, CdS particles are deliberately encapsulated into porous solid hosts of large particle size to obtain hybrid nanophotocatalysts. The widely employed supports for ulftrafine photocatalyst particles include activated carbon,[18] polypropylene granules,[19] Nafion,[20,21] resin[22] etc. Particularly, polymeric materials have been emerging as hosts of choice to obtain naocomposites partly because their attractive mechanical strength, nanoporous structure, controllable surface chemistry, and favorable interactions with the nanoparticles.[23,24]

In our recent report,[25] we employed a macroporous polystyrene anion exchanger D201 (with $-CH_2N^+(CH_3)_3$ chemically binding the polystyrene matrix) as the host and prepared a polymer-based CdS nanocomposite D201-CdS. The resultant composite photocatalyst combined excellent handling properties of the spherical D201 beads with attractive visible-light photodegradation activity of nano-CdS toward Rhodamine B (RhB). Cyclic photocatalytic reaction test indicated that photocorrosion of CdS was effectively inhibited after its encapsulation within the polymeric host, and the composite could be employed for repeated use without any significant activity loss. In addition, we examined the effect of different CdS distribution with D201 on the photoreactivity of the resultant composite.[26] Considering that different functional groups can be readily grafted on the polystyrene matrix through a simple replacement reaction, here we aimed at probing the role of polymeric surface groups in the structure and properties of nano-CdS-encapsulated composite catalysts. To achieve the goal, we encapsulated nano-CdS within three macroporous polystyrene resins D001, CP, and D201 binding $-SO_3^-$, $-CH_2Cl$, and $-CH_2N^+(CH_3)_3$ respectively, and obtained three hybrid photocatalysts denoted D001-CdS, CP-CdS, and D201-CdS. The effect of the host surface groups on CdS distribution, dispersion, crystal structure, and stability were investigated. In addition, the photocatalytic efficiency of three hybrid photocatalysts toward RhB was also examined.

2. EXPERIMENTAL SECTION

2.1. Materials. All chemicals were of analytical grade and provided by Shanghai Reagent Station. The macroporous polystyrene-divinylbenzene (St-DVB) resin in spherical beads was employed as the starting material for further surface modification, which was purchased from Zhengguang Resin Co, China. Prior to use, it was sieved to obtain narrow particle size distribution (0.6−0.8 mm in

Received: May 2, 2012
Accepted: July 10, 2012
Published: July 10, 2012

   dx.doi.org/10.1021/am300769b | ACS Appl. Mater. Interfaces 2012, 4, 3938−3943

diameter), extracted with ethanol for 6 h in a Soxhlet apparatus to remove impure residues and then dried at 60 °C for 24 h.

2.2. Synthesis of the Host Polymers. The host polymers binding different functional groups were synthesized from the St-DVB spherical beads according to the literature,[27] and three porous resins, i.e. D001 binding negatively charged sulfonate groups, CP binding neutral chloromethyl groups, and D201, binding positively charged quaternary ammonium groups, were obtained. Schematic illustration of synthesis of the polymeric hosts was available in Figure 1. The

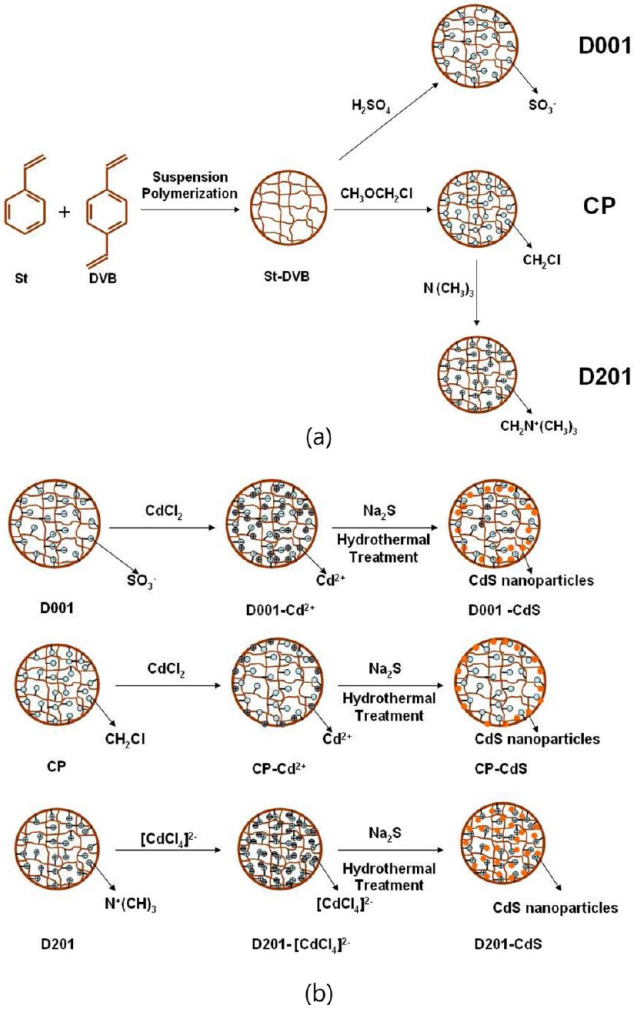

Figure 1. Schematic illustration for preparation of (a) the support polymers, and (b) the hybrid photocatalysts.

presence of functional groups binding the polymeric hosts was further demonstrated by FT-IR spectra in Figure S1 (Supporting Information). All the host polymeric beads were subjected to rinsing with NaOH (5 wt %), deionized water, HCl (5 wt %), and alcohol in a glass column in sequence, and then dried at 40 °C for further use.

2.3. Fabrication of Resin-CdS Composites. To synthesize the polymeric hybrid photocatalysts containing nano-CdS, we used $CdCl_2 \cdot 2.5H_2O$ as the cadmium source. 10.0 g of D001 and CP were immersed into 100 mL aqueous solution of 0.5 M $CdCl_2$ respectively and stirred at 30 °C for 12 h. As for D201, the $CdCl_2$ (0.5 M)-NaCl (8.0 M) binary solution were employed instead of pure $CdCl_2$ solution because the cationic Cd^{2+} cannot directly diffuse into the inner pores of D201 due to the electrostatic repulsion, and the main Cd species in the binary solution, i.e., $CdCl_4^{2-}$ can be preloaded within D201 through a typical ion-exchange process. The Cd(II)-preloaded resin particles obtained above were placed into the stainless steel autoclave attached with a Teflon tube of internal volume of 120 cm^3, and 60 mL of 1.0 M Na_2S solution were added, respectively. The autoclaves were heated and maintained at 80 °C for 24 h. The resin beads were then washed sufficiently with distilled water and dried at 40 °C to a constant weight. The schematic process for fabrication of the hybrid photocatalysts was also depicted in Figure 1.

2.4. pH-Dependent Stability of the Immobilized Nano-CdS. To investigate the effect of solution pH on the stability of CdS immobilized on the resin beads, every 0.050 g portions resin-CdS (D001-CdS, CP-CdS, D201-CdS) was immersed in 100 mL 0.50 M $Ca(NO_3)_2$ solution of different pHs adjusted by nitric acid. The suspensions were stirred at 30 °C for 48 h, and their Cd(II) content were determined by atomic adsorption spectroscope to examine the amounts of CdS leaching from the resin-CdS composites. The Cd(II) leaching into the solution could react with the sulfonate groups grafted to D001 resin through ion exchange process, Thus, 0.50 M Ca(II) was needed to screen the electrostatic attraction of the sulfonate groups according to ref.[28]

2.5. Photocatalytic Experiments. 1.00 g of D001-CdS, 2.02 g CP-CdS, or 0.78 g D201-CdS and 50 mL aqueous solution of RhB (20 mg/L) were introduced into the reactor and magnetically stirred at 60 rpm. Different amounts of the hybrid composites were deliberately selected to keep the same amount of CdS for reaction. A 350 W xenon lamp was used as the light source and a cutoff filter was equipped to block the light below 420 nm. The distance from the reactor to the light source was 5.0 cm. The parallel experiments used for comparison were carried out under identical conditions except in darkness. At given intervals, an approximate amount of solution was sampled and subject to UV−vis spectral analysis. The reactivity of the hybrid photocatalysts was assessed by monitoring the variation in RhB concentration calculated according to its absorbance at the wavelength of 553 nm.

2.6. Characterization and Analyses. The amount of CdS immobilized on the three host materials was determined by digesting the hybrid particles into a binary solution of perchloride acid and nitric acid (V:V = 7:3), followed by analysis using a atomic absorption spectrometer (TAS-990, China). The specific surface area and pore size distribution of the resin beads before and after CdS entrapment was analyzed by micropore physisorption analyzer (NOVA3000e, USA). CdS distribution within the cross section of the resin was performed on a scanning electron microscope (Hitachi S-3400N II, Japan) equipped with an energy-dispersive X-ray analyzer (Horiba EX-250 Japan). The nano-CdS dispersion within the resin matrix was observed by transmission electron microscopy (JEM-100S, Japan). Zeta potentials of the nanocomposites were obtained by using a Zeta-plus Analyzer (Brookhaven Instruments Co., USA). XRD patterns of the resin-CdS composite were recorded on an X-ray diffractometer (XRD6000, Japan).

The content of Cd(II) in solution was determined by an atomic adsorption spectroscope (TAS-990, China). UV−vis spectra of the test solutions after contacting with the composite materials under or without light irradiation were recorded by a UV−vis spectrophotometer (UV-2450, Japan). The amount of surface functional groups binding the polymeric hosts including $-CH_2Cl$, $-SO_3^-$, and $-N^+(CH_3)_3$ were determined based on the methods described by He and Huang[27]

3. RESULTS AND DISCUSSION

3.1. Effect of the Host Functional Groups on CdS Distribution. The surface distribution of elemental Cd and S in the cross-sections of the resin-CdS shown in Figure 2 clearly demonstrated that CdS immobilized on D001 and CP were distributed near the outer surface of the resin beads and formed a ring-like region, whereas CdS was uniformly distributed on D201. Such CdS distribution seems greatly dependent upon the functional groups grafted on the resin beads. It can be assumed that the electrostatic repulsion of the sulfonate groups grafted on D001 would prevent the sulfide anions further diffusing into the inner region of D001, and Cd(II) preloaded within the host

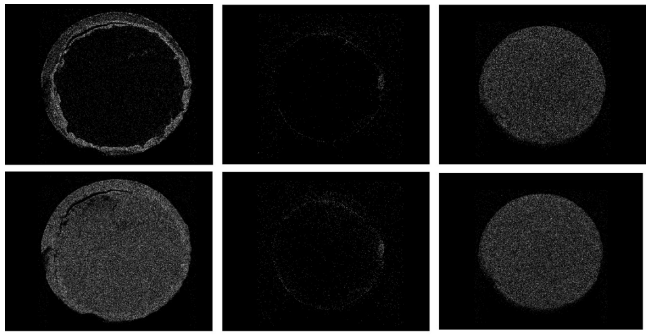

Figure 2. Surface distribution of elemental Cd (top) and S (bottom) of the cross-section of the photocatalytic composites.

matrix would diffuse to the outer region for CdS formation.[28] On the contrary, the quaternary ammonium groups uniformly distributed within D201 would react with S^{2-} through electrostatic attraction. Consequently, the sulfide anions would diffuse into the inner region of D201 until reaching equilibrium. As for CP, there is no charged functional groups grafted within the polymeric matrix, and both Cd^{2+} and S^{2-} were difficult to diffuse into the inner region of CP due to its relatively hydrophobic nature, resulting in CdS formed only near the outer surface of CP.

As seen in Table 1, the amounts of CdS immobilized on D001, CP, and D201 were 143.9, 71.4, and 185.5 mg/g, respectively. After CdS immobilization, different polymeric composites exhibit different variation in surface area. CdS encapsulation resulted in a great drop of the surface area of D201 from 25 to 10 m^2/g, while for other two hosts the surface area increased to different contents. It is understandable that CdS immobilization within porous polymers would cause considerable pore blockage. On the other side, it would possibly lead to the formation of new pores of narrower size within the polymeric hosts.[29] The above both effects would make the surface area values approach toward the opposite directions, i.e., pore blockage makes the surface area drop down while pore formation makes it increase up. Here it is just suggested that pore blockage played a dominant role in the D001-CdS composite, while pore formation might play an important role in the other two composites. However, further study is required to warrant such assumption.

3.2. Effect of Host Functional Groups on CdS Dispersions. Figure 3 depicts the TEM images of the three composite photocatalysts. In general, CdS is well-dispersed within D001 and D201 and present as nanoparticles with an average particle size <20 nm. On the contrary, a mass of aggregates were observed for CP-CdS. Given the similar pore and frame structures of three polymeric supports, it is believed that the surface functional groups grafted on the host polymers was an important factor responsible for nano-CdS dispersion,

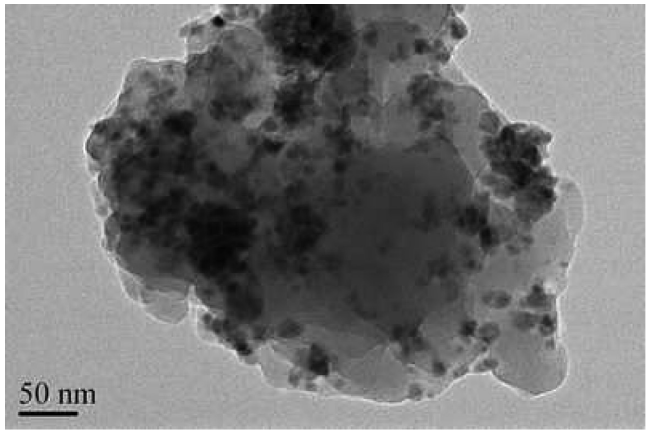

(a)

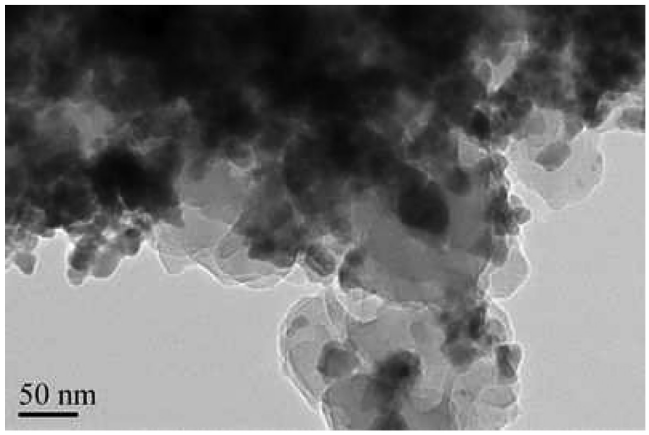

(b)

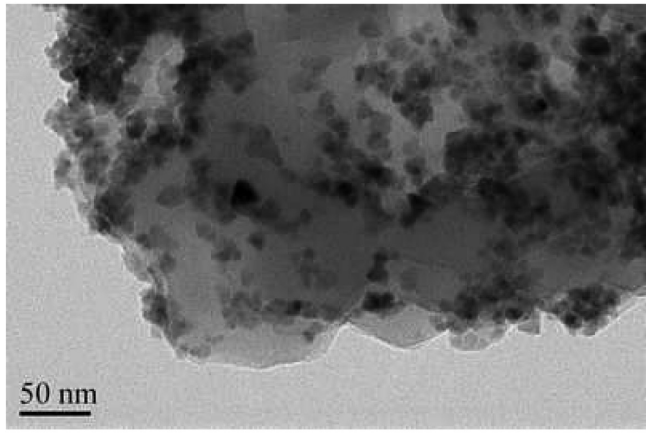

(c)

Figure 3. TEM images of composite photocatalysts (a) D001-CdS, (b) CP-CdS, and (c) D201-CdS.

Table 1. Salient Properties of the Host Polymers and the Photocatalytic Composites

designation	St-DVB	D001	D001-CdS	CP	CP-CdS	D201	D201-CdS
functional groups		$-SO_3^-$ (3.10 mmol/g)		$-CH_2Cl$ (4.81 mmol/g)		$-CH_2N^+(CH_3)_3$ (2.52 mmol/g)	
amount of CdS (mg/g)	0	0	143.9	0	71.4	0	185.5
BET surface area (m^2/g)	33.8 ± 2.3	25.2 ± 1.5	10.0 ± 0.9	32.7 ± 1.4	39.7 ± 0.8	17.0 ± 1.1	21.9 ± 1.5

and the presence of the positively (ammonium) or negatively (sulfonate) charged functional groups was more favorable than the neutral chloromethyl group to improve the nano-CdS dispersion. Similar observations were reported for immobilizing nanosized zirconium phosphate on the polymeric resins.[30] According to the DLVO theory,[31] nanoparticle stability is greatly associated with the interplay of van der Waals forces and electrostatic double-layer repulsion interaction between adjacent nanoparticles, and the double-layer repulsion generally dominates the extent of nanoparticle dispersion or aggregation. It is generally known that higher zeta potential values indicate enhanced double layer repulsion as well as preferable dispersion of nanoparticles.[32−34] The zeta potentials values of D001-CdS, CP-CdS and D201-CdS were −38.0, −20.4, and 32.4 mv respectively. The absolute zeta potentials of D001-CdS and D201-CdS higher than illuminated that the presence of the charged functional groups would enhance the double layer repulsion and consequently promote the dispersion of CdS nanoparticles.

3.3. Effect of the Host Functional Groups on CdS Structure and Stability. As shown in Figure 4, the crystal

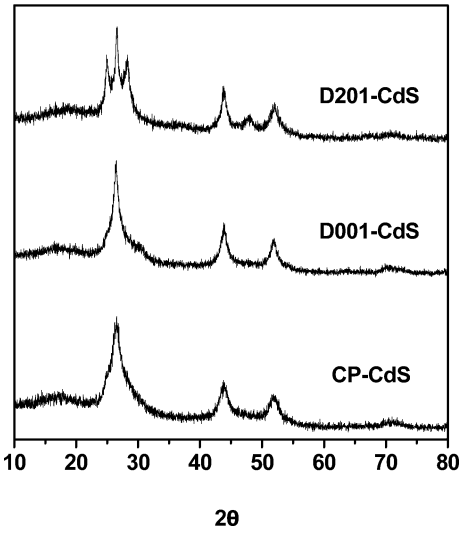

Figure 4. XRD pattern of the nanocomposite photocatalysts.

structure of CdS immobilized on D201 was hexagonal wurtzite type and that immobilized on D001 and CP were pure cubic sphalerite type. This could be explained by the concentration of Na_2S within the pores of the resin. The quaternary ammonium grafted on the polymeric matrix D201 would greatly enhance the permeation and preconcentration toward S^{2-} and then increased its concentration within the pores of the resin significantly. At a given temperature, the crystal growth and phase transformation would be promoted by increasing the concentration of Na_2S during the hydrothermal treatment,[35] i.e. the equilibrium crystal structure tends to change from the pure cubic sphalerite type to a mixture of cubic and hexagonal, and finally to the hexagonal wurtzite type. The results also indicated that a desired crystalline of CdS immobilized on the resin would be achieved by adjusting the surface functional groups grafted on the resin host.

Figure 5 describes the CdS leaching from solid particles to solution at different pHs, and it is reasonable that higher acidity corresponds to more CdS dissolution and lower CdS stability. In general, CdS nanoparticles immobilized on D201 seemed a

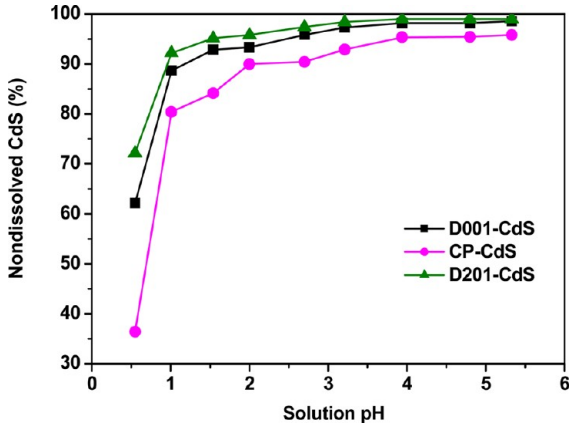

Figure 5. Effect of solution pH on Cd(II) dissolution from three hybrid photocatalysts.

little more stable than that on CP and D001 in the studied pH ranges (0.5−5.5). On account of similar pore and frame structures of three polymeric hosts, different nano-CdS stability may be associated with different H^+ concentration in the inner pores of the polymeric supports. The presence of the positively charged quaternary ammonium groups bound to the polymeric matrix D201 have an excluding effect on H^+ diffusion within the polymeric phase, leading to lower H^+ concentration in the pores of D201 than in solution. On the contrary, the sulfonate groups bound to D001 would adsorb H^+ through electrostatic attraction and result in a higher H^+ concentration in the polymeric phase than in solution. As for CP-CdS, as seen in Figure 2 and Figure 3, most of the CdS particles were coated and congregated on the outer surface of CP beads. Thus, the polymeric host of CP could not effectively protect CdS from acidic dissolution. As a consequence, CP-CdS exhibited the poorest Antiacid dissolution among three composites. .

3.4. Effect of the Host Functional Groups on the Photocatalytic Activity. As seen in Figure 6, regardless of visible light irradiation, the RhB removal efficiency of CP-CdS and D201-CdS in equilibrium is much higher than D201-CdS, and CP-CdS exhibited the fastest RhB removal kinetics, followed by D001-CdS and D201-CdS in sequence. RhB removal in darkness by the polymer-based composite could be

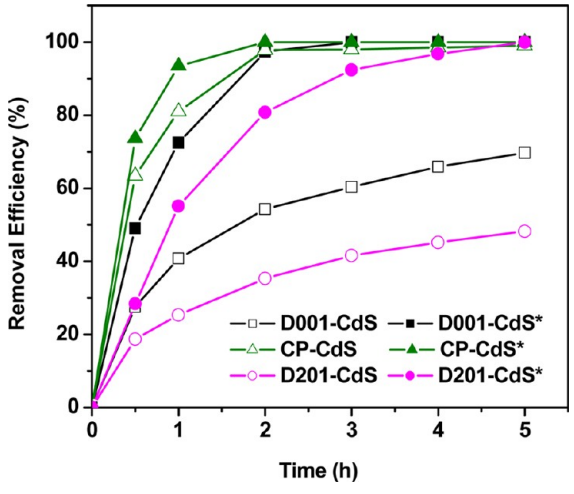

Figure 6. Time-dependent removal efficiency under (*) or without visible light irradiation (initial solution pH, 4.66).

dx.doi.org/10.1021/am300769b | ACS Appl. Mater. Interfaces 2012, 4, 3938−3943

achieved through physicochemical adsorption, because the nanoporous structure and the polystyrene nature of the host materials were proved to facilitate the adsorption process of dyes of aromatic structure through specific $\pi-\pi$ interaction and micropore filling.[36] Different removal rate is consistent with their different pore size distribution (Figure 7), and the fastest

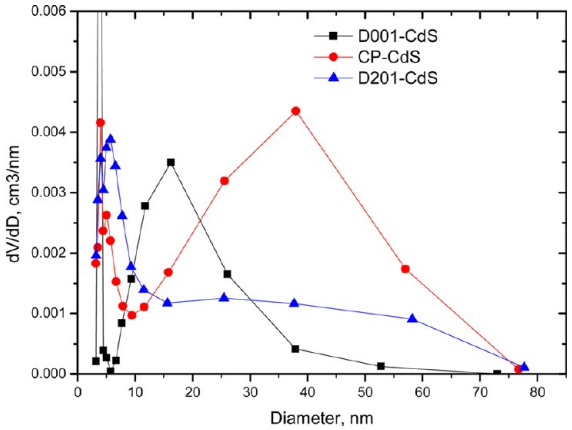

Figure 7. Pore size distribution of three CdS-loaded nanocomposites.

adsorption kinetics of CP-CdS may be associated with its widest pore size distribution in the diameter range of 5−80 nm. Also, the highest surface area of CP-CdS is also favorable for RhB adsorption capacity. As for different amounts of the adsorbed RhB for D001-CdS and D201-CdS, it is understandable because of the different electrostatic interaction between RhB and the polymeric hosts. The sulfonate groups of D001 would exhibit an electrostatic attraction toward the positively charged RhB (its molecular structure is available in Figure S2 in Supporting Information), while the quaternary ammonium groups D201 have an unfavorable effect on RhB adsorption due to the electrostatic repulsion.

To further probe the contribution of photocatalytic degradation on RhB removal, we examined the maximum absorption wavelength shifts of the test solution as a function of reaction time regardless of visible light irradiation. Previous studies[37,38] indicated that the photodegradation efficiency of RhB could be represented by the variation in maximum absorbance wavelength of the test solution, and the blue shifts of RhB solution resulted from the N-de-ethylated intermediates of RhB formed during photodegradation. From Figure 8 one can conclude that RhB photodegradation efficiency by three nanocomposites followed such an order as D001-CdS > D201-CdS > CP-CdS, which is quite different from their removal efficiency. In detail, although CP-CdS had the highest removal for RhB under visible light irradiation, its poor photodegradation toward RhB indicated that adsorption played a dominant role in RhB removal. Possibly because its RhB adsorption was so fast and strong, the adsorbed RhB inside the beads seemed inaccessible for photodegradation because most of the immobilized CdS was distributed outside the composite beads. Also, the visible light could not be available for photoreaction in the inside region of the beads, as demonstrated earlier.[26] As for higher photodegradation efficiency of D001-CdS than D201-CdS, two possible reasons should be considered except for their different crystalline structure of CdS. The first is the different electrostatic interactions between both polymeric hosts and RhB, as discussed above. The second is their different distribution of

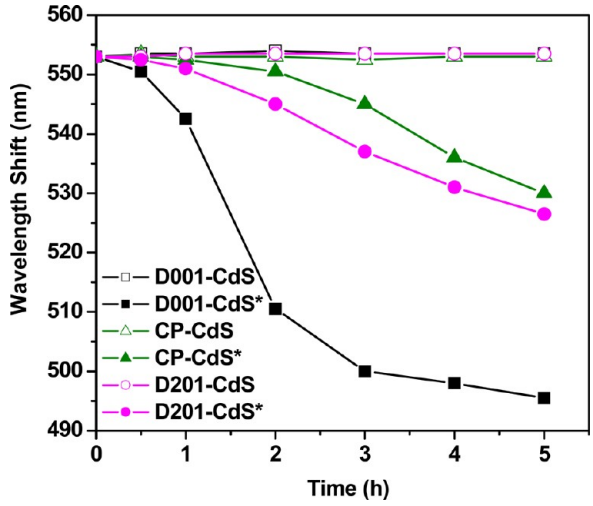

Figure 8. Maximum absorption wavelength shifts as a function of reaction time without or under visible light irradiation (*).

the loaded CdS. Our recent study demonstrated that there is a valid shell thickness of CdS for similar composite catalysts due to the limited penetration of visible light through the polymeric matrix.[26] In the valid region the density of CdS is an important factor affecting the photoreaction efficiency, and higher valid CdS density means the larger amount of CdS available for photoreaction. Apparently, though a little lower amount of CdS preloaded within D001 than D201, the valid CdS density of D001-CdS is much higher than D201-CdS because most of CdS was distributed near the outer surface of the D001 beads and formed a ringlike region, whereas it was uniformly distributed on D201.

4. CONCLUSIONS

The effect of surface functional groups of the host polymers on the performance of polymer-CdS nanocomposites was elucidated by using visible-light degradation of RhB as a case study. Our results indicated that the host surface groups greatly affected the properties of the resultant nanocomposites in terms of CdS distribution, dispersion, crystal structure, and stability, resulting in their different photocatalytic activity. These findings suggest that surface modification of the host materials possibly be an effective approach to mediate the structure and properties of the resultant nanocomposite photocatalysts.

■ ASSOCIATED CONTENT

Supporting Information

Figures S1 and S2. This material is available free of charge via the Internet at http://pubs.acs.org/

■ AUTHOR INFORMATION

Corresponding Author

*E-mail: bcpan@nju.edu.cn. Tel: +86-25-8968-0390.

Notes

The authors declare no competing financial interest.

■ ACKNOWLEDGMENTS

We acknowledge the financial support from NSFC (51008151), Jiangsu NSF (BK2011016), and Program for New Century Excellent Talents in University of China (NCET10-0489/90).

REFERENCES

(1) Mills, A.; Davies, R. H.; Worsley, D. *Chem. Soc. Rev.* **1993**, *22*, 417−425.
(2) Fox, M. A.; Dulay, M. T. *Chem. Rev.* **1993**, *93*, 341−357.
(3) Hoffmann, M. R.; Martin, S. T.; Choi, W. Y.; Bahnemann, D. W. *Chem. Rev.* **1995**, *95*, 69−96.
(4) Fernandez, A.; Lassaletta, G.; Jimenez, V. M.; Justo, A.; GonzalezElipe, A. R.; Herrmann, J. M.; Tahiri, H.; AitIchou, Y. *Appl. Catal., B* **1995**, *7*, 49−63.
(5) Minero, C.; Pelizzetti, E.; Pichat, P.; Sega, M.; Vincenti, M. *Environ. Sci. Technol.* **1995**, *29*, 2226−2234.
(6) Gao, L.; Jiang, L. Q. *Mater. Chem. Phys.* **2005**, *91*, 313−316.
(7) Gondal, M. A.; Hayat, K.; Khaled, M. M.; Ahmed, S.; Shemsi, A. M. *Appl. Catal., A* **2011**, *393*, 122−129.
(8) Wang, W. Z.; Xu, H. L.; Zhu, W. *J. Phys. Chem. B.* **2006**, *110*, 13829−13834.
(9) Rajeshwar, K.; Somasundaram, S.; Chenthamarakshan, C. R. N.; de Tacconi, N. R. *Int. J. Hydrogen Energy* **2007**, *32*, 4661−4669.
(10) Frank, A. J.; Honda, K. *J. Phys. Chem.* **1982**, *86*, 1933−1935.
(11) Ai, Z. H.; Lu, L. R.; Li, J. P.; Zhang, L. Z.; Qiu, J. R.; Wu, M. H. *J. Phys. Chem. C.* **2007**, *111*, 4087−4093.
(12) Wu, S. S.; Cao, H. Q.; Yin, S. F.; Liu, X. W.; Zhang, X. R. *J. Phys. Chem. C.* **2009**, *113*, 17893−17898.
(13) Ashokkumar, M.; Maruthamuthu, P. *J. Photochem. Photobiol. A* **1989**, *49*, 249−258.
(14) Quan, X.; Guo, Y. F.; Lu, N.; Zhao, H. M.; Chen, S. *Environ. Sci. Technol.* **2007**, *41*, 4422−4427.
(15) Fu, H. B.; Pan, C. S.; Yao, W. Q.; Zhu, Y. F. *J. Phys. Chem. B* **2005**, *109*, 22432−22439.
(16) Linsebigler, A. L.; Lu, G. Q.; Yates, J. T. *Chem. Rev.* **1995**, *95*, 735−758.
(17) Meissner, D.; Memming, R.; Kastening, B. *J. Phys. Chem.* **1988**, *92*, 3476−3483.
(18) Lee, J.; Suh, J.; Hong, J.; Lee, Y.; Park, J. *Carbon* **2008**, *46*, 1648−1655.
(19) Han, H.; Bai, R. *Ind. Eng. Chem. Res.* **2009**, *48*, 2891−2898.
(20) Liu, P.; Wang, J. C.; Fu, X. Z.; Li, Z. H.; Han, W.; Wang, X. X. *Langmuir* **2009**, *25*, 1218−1223.
(21) Wang, S.; Liu, P.; Wang, X.; Fu, X. *Langmuir* **2005**, *21*, 11969−11973.
(22) Wang, M.; Wang, C.; Wang, W. *Mater. Chem. Phys.* **2007**, *104*, 162−165.
(23) Keledi, G.; Hári, J.; Pukánszky, B. *Nanoscale* **2012**, *4*, 1919−1938.
(24) Zhao, X.; Lv, L.; Pan, B. C; Zhang, W. M; Zhang, S. J.; Zhang, Q. X. *Chem. Eng. J.* **2011**, *170*, 381−394.
(25) Xie, Y. M.; Lv, L.; Zhang, S. J.; Pan, B. C.; Wang, X. S.; Chen, Q.; Zhang, W. M.; Zhang, Q. X. *Nanotechnology* **2011**, *22*, 305707.
(26) Xie, Y. M.; Zhang, S. J.; Pan, B. C.; Lv, L.; Zhang, W. M. *Chem. Eng. J.* **2011**, *174*, 351−356.
(27) He, B. L. Huang, W. Q.; *Ion Exchanger and Adsorptive Resin*; Science Technology Education Press:Shanghai, 1995.
(28) Xie, Y. M.; Lv, L.; Li, M. H.; Pan, B. C.; Chen, Q.; Zhang, W. M.; Zhang, Q. X. *Sci. China Chem.* **2012**, *55*, 409−415.
(29) Jiang, Z. M.; Lv, L.; Zhang, W. M.; Du, Q.; Pan, B. C.; Yang, L.; Zhang, Q. X. *Water Res.* **2011**, *45*, 2191−2198.
(30) Zhang, Q. R.; Pan, B. C.; Zhang, S. J.; Wang, J.; Zhang, W. M.; Lv, L. *J. Nanopart. Res.* **2011**, *13*, 5355−5364.
(31) Behrens, S. H.; Christl, D. I.; Emmerzael, R.; Schurtenberger, P.; Borkovec, M. *Langmuir* **2000**, *16*, 2566−2575.
(32) Guzman, D.; Katherine, A.; Finnegan, M. P.; Banfield, J. F. *Environ. Sci. Technol.* **2006**, *40*, 7688−7693.
(33) Mukherjee, B.; Weaver, J. W. *Environ. Sci. Technol.* **2010**, *44*, 3332−3338.
(34) Mulvihill, M. J.; Habas, S. E.; Jen-La Plante, H.; Wan, J. M.; Mokari, T. *Chem. Mater.* **2010**, *22*, 5251−5257.
(35) Lin, Z.; Xiong, Y. S.; Zhang, J.; Huang, F.; Ren, G. Q.; Liu, W. Z.; Li, D. S.; Wang, C. *J. Phys. Chem. C.* **2008**, *112*, 9229−9233.
(36) dos Reis, L. G. T.; Robaina, N. F.; Pacheco, W. F.; Cassella, R. J. *Chem. Eng. J.* **2011**, *171*, 532−540.
(37) Watanabe, T.; Takizawa, T.; Honda, K. *J. Phys. Chem.* **1977**, *81*, 1845−1851.
(38) Yu, K.; Yang, S. G.; He, H.; Sun, C.; Gu, C. G.; Ju, Y. M. *J. Phys. Chem. A* **2009**, *113*, 10024−10032.